

ELECTRONIC PROPERTIES OF Cu-As-Se GLASSESV.I. MIKLA^{a*}, A.A. KIKINESHI, V.V. MIKLA^b, D.G. SEMAK^a Institute for Solid State Physics and Chemistry, Uzhgorod National University,
Uzhgorod, Voloshina 54, Ukraine^b Yazaki, Ukraine, LtdCorresponding author: mikla@univ.uzhgorod.ua**Abstract**

Fundamental physical properties of Cu-As-Se glasses along Cu-As₂Se₃ tie lines have been investigated in order to obtain information on electronic structure. Progressive Cu addition to As₂Se₃ induces gradual red shift of the absorption edge and significantly reduces the value of dark conductivity and its activation energy. The latter is also confirmed by the thermally stimulated depolarization current experiments. Taken together, all of the data including steady state photoconductivity measurements indicate that the “electrical” and “optical” band gap gradually narrowed with Cu addition. It is established that Cu addition in As-Se glasses causes a significant change in the dark conductivity value and its activation energy. Cu-As-Se glasses are photoconductive and the temperature dependence behaves in a usual manner and, below the maximum, shows the corresponding slope in the low temperature region. Thermally stimulated currents were also present in these materials. On the basis of these observations, electronic structure of Cu-As-Se is considered from the point of view of Mott-Davis model.

(Received December 28, 2008; accepted February 6, 2009)

Keywords: Cu-As-Se; Chalcogenide; Thermally stimulated currents; Electronic Properties; Trap level; Amorphous Semiconductors

1. INTRODUCTION

Although the physical properties and electronic structure of elemental selenium and Se-based binary glasses have been investigated extensively, little is known about electronic structure of ternary chalcogenides. The latter is especially true for the case of Cu alloying with As₂Se₃; the fundamental properties of ternary Cu-As-Se glasses were fragmentary [1-10]. At the same time, Cu-As-Se glasses can be used for optical data storage and in various technical devices [10].

In the present paper, some fundamental properties (e.g. DC conductivity, photoconductivity, thermally stimulated currents and direct structural probe via X-ray diffraction) have been investigated for knowledge of electronic structure of Cu-As₂Se₃ glasses. Based on the experimental results, we have proposed simple model for influence of copper addition on electronic states localized in the band-gap of As₂Se₃.

EXPERIMENTAL

Bulk samples were made by mixing pure elements and loading them into clean quartz ampoules (inner diameter 8 mm). Ampoules were then sealed under a vacuum of 10^{-6} Torr. The $\text{Cu}_x(\text{As}_x\text{Se}_{1-x})_{100-x}$ ingots were kept at 950 °C for about 80 h in a rocking furnace, and then cooled down to 850 °C, followed by quenching in air (compositions $0 \leq x \leq 30$ at.%) to room temperature. Note that these compositions were from the glass-forming region reported by Borisova [8]. Powder X-ray diffraction spectra were taken to ensure that there were no crystalline inclusions in the samples.

The bulk samples were obtained in a usual manner and then polished with diamond powder and pastes. For measurements of DC conductivity, the samples have the shape of platelets typically $2 \times 2 \times 0.5$ mm² size. As electrodes, vacuum thermally evaporated gold electrodes were used. Experimental details for the measurements of DC conductivity, photoconductivity and other electrical measurements the reader may find in our earlier paper [3].

The optical absorption coefficients of the glasses were obtained through the measurement of the spectral dependence of the optical transmittance, T . The sample thickness, d , was varied from 100 μm to 1 mm. The absorption coefficient, α , was calculated using the following formula

$$T = (1 - R)^2 \exp(-\alpha d), \quad (1)$$

where R is the reflectivity, which is evaluated from the transmittance ($\sim 60\%$) in the near infrared region.

For Urbach tails to be investigated quantitatively, α , the absorption coefficient, in these regions is described by an exponential function, $\alpha \sim \exp(h\omega/kT_u)$, where T_u is the characteristic temperature in the Urbach region.

2. STRUCTURE

Typical X-ray diffraction patterns in $\text{Cu}_x(\text{As}_x\text{Se}_{1-x})_{100-x}$ glasses are shown in Fig. 1. We start with As_2Se_3 . Three halo peaks are clearly seen in the patterns of As_2Se_3 , namely the characteristic first sharp diffraction peak (FSDP) located at $2\theta \sim 17^\circ$ which is attributed to medium range structural order, and the second and the third peaks, located at $2\theta \sim 30^\circ$ and $2\theta \sim 52^\circ$, respectively.

The latter peaks are due to the correlations between the second nearest neighbors and between the nearest neighbors. When alloying As_2Se_3 with Cu, we observe the following effects: a) FSDP weakening and even disappearing at $x > 15$; b) additionally, the peaks at $2\theta \sim 30^\circ$ and $2\theta \sim 52^\circ$ shifting to lower angles when Cu content increases. Here we note that these changes are in accordance with studies by Liang [6] and Itoh [4].

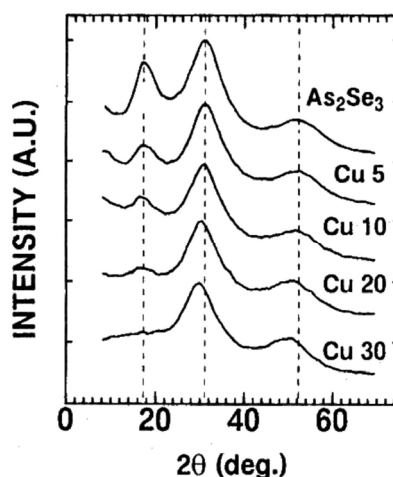


Fig. 1. X-ray diffraction patterns obtained for Cu-As-Se glasses. The intensities are normalized by the peaks at $2\theta \sim 30^\circ$. Cu content is shown for each curve.

It is well established that amorphous chalcogenide semiconductors have short-range order very close to their crystalline analogs [6,11]. Thus, it seems reasonable to compare their diffraction patterns. Fig. 2 shows the result of such a comparison between the diffraction patterns of $g\text{-As}_2\text{Se}_3$ and $g\text{-Cu}_{30}\text{As}_{28}\text{Se}_{42}$ with powder diffraction patterns of their crystalline counterparts' $c\text{-As}_2\text{Se}_3$, $c\text{-CuAsSe}_2$ and $c\text{-Cu}_3\text{AsSe}_3$. As can be clearly seen, all of the three halo peaks in $g\text{-As}_2\text{Se}_3$ are located at the positions where intense diffraction peaks in $c\text{-As}_2\text{Se}_3$ are observed (this experimental fact was reported firstly by Vaipolin and Porai-Koshits [9]). In addition, one can see that the positions of the halo peaks in Cu-As-Se ternary glasses are close to diffraction peaks in the Cu-As-Se crystals [6,11]. It is important to note that Cu-As-Se, being in crystalline or non-crystalline forms, exhibit no diffraction peak at $2\theta \sim 17^\circ$, which is inherent to the FSDP of glassy As_2Se_3 .

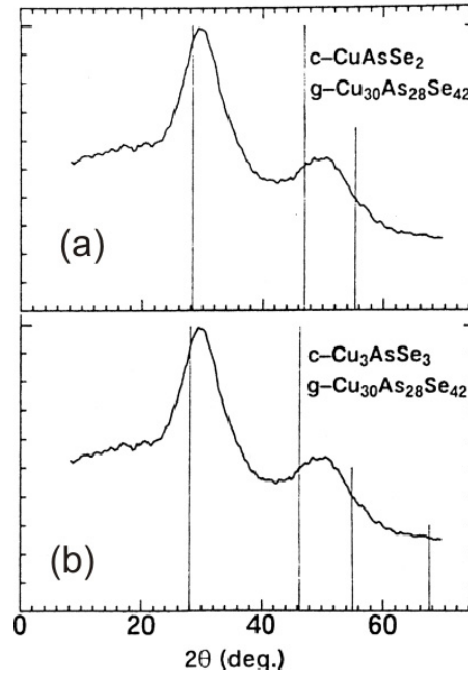


Fig. 2. X-ray diffraction patterns of glassy and crystalline Cu-As-Se.

Summarizing the above diffraction experimental results and taking into account diffraction data on the corresponding crystals, we may assume remarkable features of Cu-As-Se glasses structure depending on the Cu content: a) Cu-As-Se ternary glasses with Cu content less than 15 at% exhibit three halo diffraction peaks similar to that in As_2Se_3 and this means the preservation of short- and medium- range order; b) at the same time, for $x > 15$ at%, two halo peaks in the diffraction patterns of Cu-As-Se glasses undoubtedly indicate the presence of crystalline phase in short-range order; c) structural units at short- and medium-range intervals are different for $x < 15$ at% and $x > 15$ at%, respectively.

3. ELECTRONIC PROPERTIES

The temperature dependence of DC (dark) conductivity for $Cu_x(As_xSe_{1-x})_{100-x}$ glasses plotted as $I(T) \sim f(10^3/T)$ is shown in Fig. 3. Clearly seen that the DC conductivity can be written in the form

$$\sigma = \sigma_0 \exp(-E_\sigma/kT). \quad (2)$$

Here σ_0 is the so-called pre-exponential factor and E_σ the activation energy. σ_0 value is approximately $10^2 \text{ Ohm}^{-1}\text{cm}^{-1}$ and suggests conductivity determined by the transport states. The DC conductivity value σ and its activation energy E_σ in $Cu_x(As_xSe_{1-x})_{100-x}$ glasses

gradually decreases with Cu content. The dependence of E_σ (together with other parameters) on copper content is reflected in Table 1.

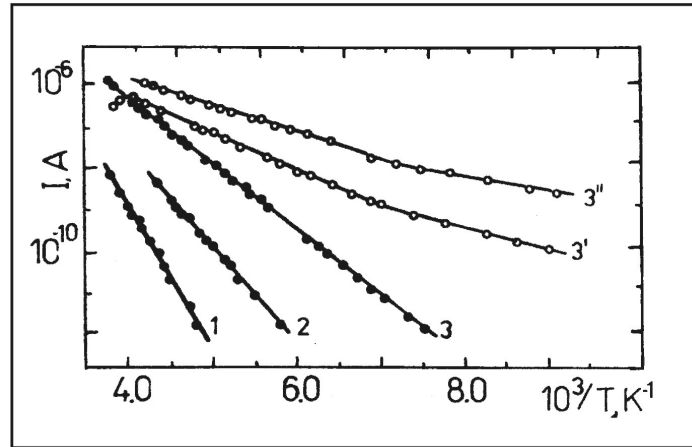


Fig. 3. Temperature dependence of DC conductivity of $\text{Cu}_x(\text{As}_2\text{Se}_3)_{1-x}$ glasses. Cu content is 5, 10 and 15 at% (curves 1-3, respectively). Also shown are the temperature dependencies of photocurrent for samples under illumination with power density $0.06 P_{\max}$ ($3'$) and P_{\max} ($3''$) ($P_{\max} \approx 4 \times 10^{-2} \text{ W/cm}^2$).

Conventional thermally stimulated currents (TSC) and thermally stimulated depolarization currents (TSDC) were shown in Figs. 4 and 5.

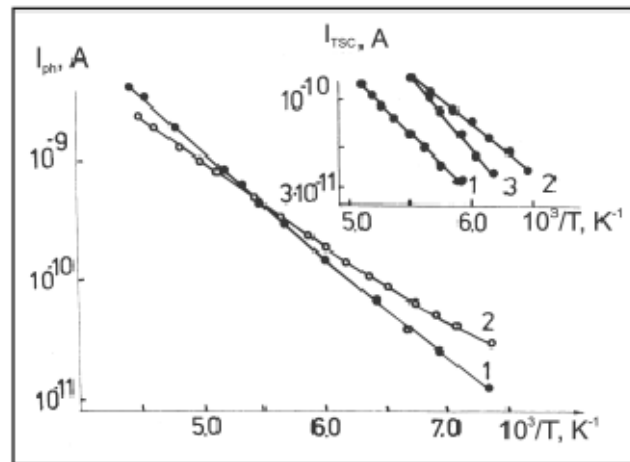


Fig. 4. Temperature dependencies of photocurrent for $\text{Cu}_x(\text{As}_2\text{Se}_3)_{1-x}$ ($x = 10$ at%) / at $P = P_{\max}$. 1 – virgin sample, 2 – pre-irradiated sample during $t_i = 30$ min with P_{\max} at $T = 100$ K. In the inset the initial part of TSC is shown: 1 – irradiation at $T = 100$ K with P_{\max} , $t_i = 1$ min; 2 – irradiation at $T = 100$ K with P_{\max} , $t_i = 30$ min; 3 – irradiation during cooling the sample from $T = 300$ K to $T = 100$ K.

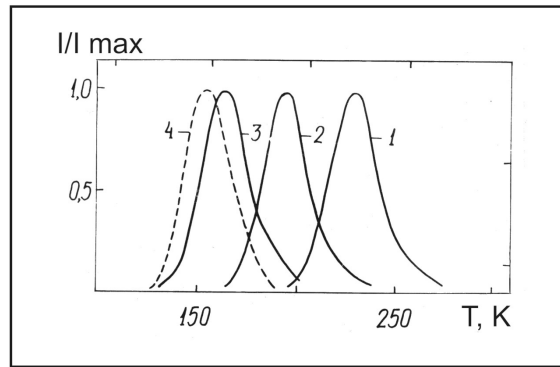


Fig. 5 Thermally stimulated depolarization in $\text{Cu}_x(\text{As}_2\text{Se}_3)_{1-x}$. Cu content: 5 at% (1); 10 at% (2); 15 at% (3). Also shown is the depolarization curve (4) for sample photopolarized at $T = 100$ K.

From the slope of the initial part of corresponding curves the activation energy E_t and E_{TSDC} were determined. Here we note that E_σ and E_{TSDC} correlate indicating that the charge carrier transitions in both cases were identical. This means, as we have shown earlier [12], that in the process of measuring TSDC one simply observed only the capacitor discharge due to DC conductivity increasing with temperature. The reader may find the detailed explanation of this problem in excellent review by Agarwal [13]. The capacitor under consideration consists of the metallic electrodes, insulating sheets and the sample (sandwich-like configuration). At the same time, even in this case, TSDC can give information about $E_\sigma \approx E_{\text{TSDC}}$, especially when difficulties in satisfactory contact realization arise. The TSDC maximum shifts to lower temperatures accordingly to E_σ decreasing (Fig. 5). Therefore, TSDC may be used as contact-free method for determination of conductivity activation energy E_σ . Only in the case when one faced with filling of the traps with non-equilibrium charge carriers, the TSDC contains information on localized band-gap states.

We conclude from the study of TSC (in conventional mode and at conditions of persistent internal polarization) that near the valence band tail states exist at E_t energy respectively to mobility edge. The comparison of the corresponding activation energy values is possible for the glasses containing less than 5 at% Cu – only these compositions exhibit distinct maximum on the depolarization curve (see Fig. 5). On the contrary, in $\text{Cu}_x(\text{As}_2\text{Se}_3)_{1-x}$ glasses with Cu content more than 5 at%, due to increased influence of equilibrium (dark) conductivity, difficulties arise in measuring depolarization curves in previously photopolarized samples. In addition, we have observed some light-induced effects on electronic properties. For example, activation energies E_a determined from TSC and TSDC curves for samples illuminated by band-gap light at 100 K were found to be lower in

comparison with E_t (Fig.4, inset) when thermo-stimulated curves were measured after standard procedure. Similar changes were observed when investigating temperature dependence of photoconductivity.

The temperature dependence of photocurrent in glasses under study consists of three regions: pre-exponential region at low-temperature; exponential rise

$$I_{ph} = A \exp(- E_{ph}/kT) \quad (3)$$

(A – const., E_{ph} – activation energy of photoconductivity determined from the slope of the corresponding dependence); and the maximum at “high” temperatures.

As expected, the absorption edge has typical for chalcogenide glasses shape and the absorption coefficient can be described by the dependence

$$\alpha \sim \exp(h\omega/kT_U), \quad (4)$$

where T_U is reciprocal of slope of absorption coefficient. The addition of Cu to As_2Se_3 or, in other words, alloying As_2Se_3 with Cu for compositions studied is accompanied by three types of effects. The first one is an increase in the absorption coefficient value. Next, after initial slight decrease in the slope of the above dependence comparing to As_2Se_3 this parameter remains unchanged independently of Cu content. That is T_U remains constant in the range 5÷30 at%. Finally, we observe a gradual shift of absorption edge to lower energies with increasing copper content. It is important to note that the rate of decrease of the activation energy E_σ is larger than that of optical gap E_g .

Table 1: Activation energies of DC conductivity E_σ , thermally stimulated depolarization current E_{TSDC} , photoconductivity E_{ph} , and trapping states depth E_t in $Cu_x(As_2Se_3)_{1-x}$ glasses.

Cu content, at %	E_σ , eV	E_{TSDC} , eV	E_{ph} , eV	E_t , eV
0	0.90	0.90	0.31	0.40
5	0.60	0.60	0.29	0.40
10	0.45	0.41	0.24	0.36
15	0.33	0.33	0.30	0.30

In Fig. 6 the energy differences between the Fermi level, from one side, and trapping states and mobility edge, from the other side, are shown. In the same Figure parameter δ represents the range of localized tail states. In other words, it may be a measure for a width of the valence band tail. In the Cu-As-Se system, δ falls with Cu introduction. This indicates that copper addition narrows the valence band tail.

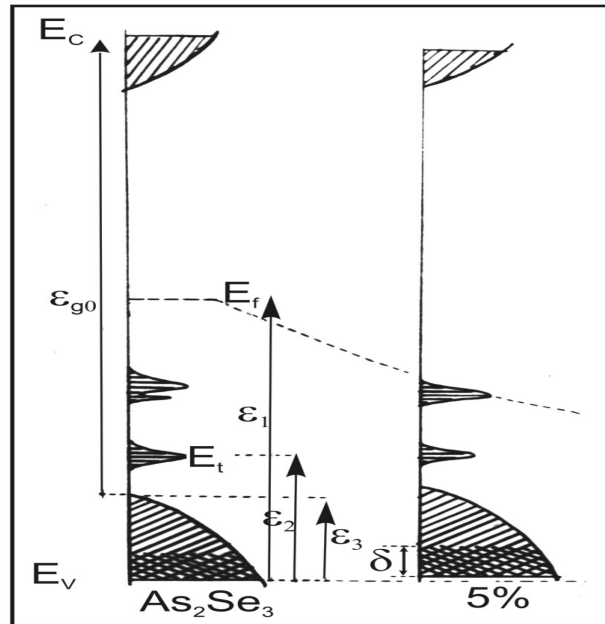


Fig. 6. Gap-states distribution in As_2Se_3 and $Cu_x(As_2Se_3)_{1-x}$ glasses (the latter is exemplified for 5 at% Cu).

5. DISCUSSION

First of all, before discussing the experimental results presented, it should be emphasized on two essential facts. These are: a) the decrease in band-gap energy with increasing Cu content in Cu-As-Se system; b) in the system considered “optical” band-gap energies were greater than estimated from conductivity measurements, $E_g > 2E_\sigma$.

For experimental results to be explained, the modified Mott-Davis model seems to be appropriate. Schematically the model is illustrated in Fig. 6. Additionally to the tails close to the mobility edges, the density of states contains several peaks. These correspond to states localized in the mobility gap. The energy interval between E_f , E_t etc. and E_v are clearly seen from Fig. 6. The activation energy of the photoconductivity below the maximum in the model determines the width of the region of states localized in the tails of the corresponding bands. Another possible explanation is that E_{ph} may be attributed to some defect states. The change in E_{ph} decreases with Cu content. In terms of the model we proposed this means that

the width of tail states also decreases. It is important to note here the correlation in E_t and E_{ph} change with increasing Cu content in $Cu_x(As_2Se_3)_{1-x}$ glasses. In other words, the peak in the density of states (traps) is the same for the range of copper concentration studied. It is assumed that this peak will overlap with states localized near Fermi level at increasing Cu concentration. Probably, this is the reason that one can observe only one set of shallow traps in glasses with $E_\sigma < 0.7$ eV. The influence of pre-irradiation (photoinduced changes of physical parameters) on the spectrum of localized states, as we believe, is similar to the effect of Cu addition to As_2Se_3 . The width of tail states decreases in both cases. The results of thermally stimulated conductivity and temperature dependence of photoconductivity support this suggestion. Liu and Taylor [7] have found that the magnitude of photodarkening effect (PD) decreases very rapidly with increasing Cu concentration and that the PD effect is eliminated in $Cu_x(As_2Se_3)_{1-x}$ for $x \geq 5$ at.%. However, in the present article we will not consider photodarkening effect and the accent is on light-induced electronic effects.

Amorphous As_2Se_3 containing copper exhibits much larger value of hole drift mobility value comparing with that of electrons (note that we cannot detect electron transient signal even for 0.1at% Cu). This may be a strong argument in favor that E_σ reflects the energy difference between the valence band mobility edge and the Fermi level.

The fact that for the compositions studied E_g values are significantly greater than $2E_\sigma$ can be explained as follows: a) copper addition shifts the Fermi level to the valence band; b) the mobility edge of the valence band shifts to higher energies; c) simultaneous effect – mutual shift of Fermi level and, respectively, mobility edge – “attractive” effect.

In the concentration region studied both E_σ and E_g decrease with increasing copper content but the more significant change is inherent to E_σ . Such a behavior may be explained by the appearance of acceptor-like states, which is induced by alloying effect.

In addition, it should be mentioned the possibility of changing the valence band tail with Cu addition. For this effect to be accounted, we adopt here the mechanism proposed by Itoh [4]. In accordance with this mechanism Cu atoms added to As-Se may interact with As-Se network, since the Cu atoms possess the 3d orbital's which effectively overlap the Se 4p orbitals. Hence, if Cu-Se bonds are assumed to be stronger than As-Se in Cu-As-Se, the Cu atoms may attempt to attract the Se atoms to form optimum Cu-Se covalent configurations. Thus, structural randomness in the Cu-Se bonding configurations may decrease with increasing structural randomness in the As-Se network. Probably, this is the reason that Cu introduction narrows the valence band tail. Additional argument in favor of this effect is that T_U (in the expression for absorption coefficient) being the measure of the tail state width

decreases with Cu addition. Note that in the present article the authors consider only the width of band tail without appealing to its concrete shape, e.g. exponential, etc.

We considered the band structure of Cu-As-Se glasses in the following way. Studies performed [4,6] to clarify the local environment around Cu atoms in Cu-As-Se glasses have shown its bonding to Se atoms with coordination numbers of 2 to 4. It seems important to note that Cu 3d bands are energetically close to the Se 4p bands. These constitute the top of the valence band in the “host” (As_2Se_3) material. In such a case the d bands will interact with Se 4p band forming d-p bonding and d-p anti-bonding states in the upper valence region. As a result, we have the situation when the top of the valence band will shift to the Fermi level (see Fig. 6). Reasonably, band-gap energies as well as the energies of gap states (traps) decrease. In the frame of this model, we have supposed that bottoms of conduction bands in Cu-As-Se glasses consist of As-Se anti-bonding states.

Finally, the nature of the Cu-Se bonds in Cu-As-Se glasses may be regarding as covalent [4]. In such a case a covalent nature of the Cu-Se, probably, explain the absence of Cu^+ ion migration studied by authors [14].

6. CONCLUSIONS

Fundamental physical properties of Cu-As-Se glasses along Cu- As_2Se_3 tie lines have been investigated in order to obtain information on band-gap structure. These physical properties can be explained from the point of view that alloying As_2Se_3 with Cu lead to progressive decreases both of the “optical” and “electrical” band-gap. The latter decrease more rapidly indicating that the valence band edge shifts to the Fermi level.

In the mobility gap of As_2Se_3 there exist a set of trapping levels located at 0.4 eV which is insensitive to copper addition. The width of valence band localized tail states is determined as activation energy from the temperature dependence of photoconductivity. Experimental results show that the width of valence band tail states decreased respectively to that in As_2Se_3 with copper addition as well as with pre-irradiation of the samples.

REFERENCES

1. N.F.Mott and E.A.Davis, *Electronic Processes in Non-Crystalline Materials*. (Clarendon. Oxford. 1979).
2. M.Kitao, H.Akao, T.Ishikawa and S.Yamada, *Physica Status Solidi (a)* 64 (2006) 493.
4. A.A.Kikineshi, V.I.Mikla, D.G.Semak, *Ukrainian J. Phys.* 23 (1978) 63.

5. M.Itoh, *J. Non-Cryst. Solids* 210 (1997) 178.
6. M.Ohto and K.Tanaka, *J. Non-Cryst. Solids* 227 (1998) 784.
7. K.S.Liang, A.Bienenstock and C.W.Bates, *Phys. Rev. B* 10 (1974) 1528.
8. J.Z.Liu and P.C.Taylor, *Phys. Rev. B* 41 (1990) 3163.
9. Z.U.Borisova. *Glassy Semiconductors* (Plenum, New York, 1981).
10. A.A.Voipolin and E.A.Porai-Koshits, *Sov. Phys. Solid State* 5 (1963) 497.
11. Y.Asahara and T.Izumitani, *J. Non-Cryst. Solids* 16 (1974) 407.
12. L.G.Berry, ed. *Powder Diffraction File* (Joint Committed on Powder Diffraction Standards, Philadelphia. PA, 1974).
13. A.A.Kikineshi, V.I.Mikla and I.P.Mikhalko, *Sov. Phys. Semicond.* 11 (1977) 1010.
14. S.C.Agarwal, *Phys. Rev. B* 10 (1974) 4340.
15. Y.G.Vlasov and E.A.Bychkov, *Solid State Ionics* 14 (1984) 329.